

# Ethanol Steam Reforming for Hydrogen Production over Bimetallic Pt–Ni/Al<sub>2</sub>O<sub>3</sub>

Enis Örüçü · Feyza Gökaliler · A. Erhan Aksoylu ·  
Z. Ilse Önsan

Received: 17 July 2007 / Accepted: 4 September 2007 / Published online: 20 September 2007  
© Springer Science+Business Media, LLC 2007

**Abstract** Ethanol steam reforming was studied at 673–823 K over Pt–Ni/ $\delta$ -Al<sub>2</sub>O<sub>3</sub>. Results indicate that bimetallic catalyst is resistant to coke deposition at steam-to-carbon ratios as low as 1.5 and higher ratios are beneficial for both ethanol conversion and hydrogen formation. About 773 K is the optimum since high H<sub>2</sub> production rates are accompanied by low CO and CH<sub>4</sub> production rates. A power-function rate expression obtained on the basis of intrinsic rates at 673 K gives reaction orders of 1.25 ( $\pm 0.05$ ) and  $-0.215$  ( $\pm 0.015$ ) for ethanol and steam, respectively; the apparent activation energy is calculated as 39.3 ( $\pm 2$ ) kJ mol<sup>-1</sup> between 673 and 723 K.

**Keywords** Ethanol steam reforming · Hydrogen production · Bimetallic catalysts · Pt–Ni

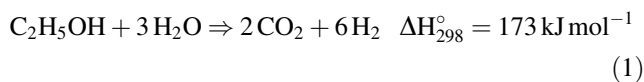
## 1 Introduction

One of the novel alternatives for clean energy generation is fuel cell technology. Polymer electrolyte membrane fuel cells (PEMFC) powered by hydrogen are well-suited for both vehicular and decentralized stationary facilities such as combined heat and power generation for houses and small-scale commercial applications [1, 2]. Since PEMFC operation requires a continuous supply of hydrogen, the use of an in situ catalytic fuel processor that will readily convert hydrocarbon fuels into hydrogen is a potentially feasible solution. Steam reforming (SR) is investigated in this context, since it has the highest efficiency for hydrogen

production. Endothermic nature of steam reforming constitutes its main drawback given that an external source of heat is needed [3, 4].

The criteria for the selection of the optimal hydrocarbon source for small-scale energy production include either a well-established distribution network, as in the case of natural gas, and/or a liquid fuel for easy storage and transportation, as in the case of gasoline. Although natural gas, gasoline and methanol are usually mentioned as the likely sources for hydrogen production, their use does not reduce reliance on fossil fuels or emission of pollutants. Ethanol has recently received attention as a hydrogen source due to its crucial advantage of being producible from renewable sources such as biomass, plants or waste materials of agricultural and forestry industries. Hydrogen production from bio-ethanol offers a nearly closed carbon loop since the carbon dioxide produced is consumed for biomass growth [5]. Ethanol is widely available, easily transportable, safe to handle and less toxic compared to methanol. Higher temperatures (573–873 K) are required for ethanol SR because of its C–C bond, and this is the only disadvantage to be tackled.

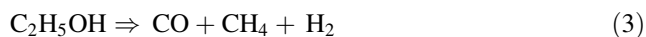
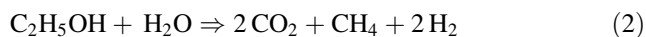
Ethanol steam reforming is a highly endothermic reaction:



Even though the overall steam reforming reaction looks straightforward, the reaction scheme is complicated by the presence of other reactions occurring in the system, depending mostly on reaction temperature and catalyst composition and resulting in exit streams containing hydrogen, carbon monoxide, carbon dioxide, methane, ethylene, acetaldehyde etc [6, 7]. The most likely side

E. Örüçü · F. Gökaliler · A. E. Aksoylu · Z. I. Önsan (✉)  
Department of Chemical Engineering, Boğaziçi University,  
Bebek, Istanbul 34342, Turkey  
e-mail: onsan@boun.edu.tr

reactions over Ni-based catalysts are ethanol SR with methane production, ethanol decomposition and methane SR:



Methanation of carbon oxides may also be considered as a possibility. Comas et al. [7] studied ethanol SR over Ni/Al<sub>2</sub>O<sub>3</sub> at 573–773 K to propose a reaction scheme. Fatsikostas and Verykios [8] investigated the effect of using different supports for Ni catalysts and reported that carbon deposition is significantly reduced by impregnating  $\gamma$ -Al<sub>2</sub>O<sub>3</sub> with La<sub>2</sub>O<sub>3</sub>. Sun et al. [9] suggested that ethanol steam reforming on Ni catalysts is first-order with respect to ethanol and computed apparent activation energies between 1.87 and 16.88 kJ mol<sup>-1</sup> depending on the type of catalyst support. Akande et al. [10] studied crude ethanol SR over Ni/Al<sub>2</sub>O<sub>3</sub> and suggested a reaction order of 0.43 with respect to ethanol and activation energy of 4.41 kJ mol<sup>-1</sup>. Although ethanol SR has recently received more attention, extended parametric and kinetic studies are scarce [11]. Intrinsic kinetics of ethanol SR studied over Ru/Al<sub>2</sub>O<sub>3</sub> using excess water, on the other hand, showed that ethanol conversion was directly proportional to ethanol partial pressure and independent of steam partial pressure with apparent activation energy of 96 kJ/mol [12].

The fuel processor/fuel cell system proposed by Avci et al. [13] for hydrogen production from different hydrocarbons was modified to investigate ethanol conversion to hydrogen by a series of thermodynamic analyses and computer simulations [14]. Hydrogen production was considered to occur over a bimetallic catalyst (such as Pt–Ni) by indirect partial oxidation (IPOX) which combines steam reforming and total oxidation reactions as well as water–gas shift (WGS) as a beneficial side reaction. In IPOX, the external energy demand of endothermic SR is minimized by the highly exothermic total oxidation. The thermodynamic approach was used, because suitable rate equation(s) for ethanol SR are lacking. The results indicated that H<sub>2</sub> yields up to 65% of the theoretical (1 mol ethanol can yield up to 6 mol H<sub>2</sub>) can be obtained with an ethanol total oxidation conversion of about 13% at a steam-to-carbon ratio of 3.3 and an IPOX reactor exit temperature of 873 K [14].

The present work focuses on ethanol SR over bimetallic Pt–Ni/ $\delta$ -Al<sub>2</sub>O<sub>3</sub>, which is a successful IPOX catalyst that has potential for fuel processor applications associated with PEM fuel cells [15, 16]. A parametric study was conducted to reveal the effects of water-to-ethanol ratio and

temperature on ethanol conversion and hydrogen formation, and a kinetic study was carried out in order to propose a power-function rate expression for ethanol conversion by steam reforming over Pt–Ni/ $\delta$ -Al<sub>2</sub>O<sub>3</sub>.

## 2 Experimental

### 2.1 Catalyst Preparation

$\delta$ -Al<sub>2</sub>O<sub>3</sub> was used as support material because of its thermal stability and suitable total surface area. Bimetallic 0.2 wt%Pt–15 wt%Ni/ $\delta$ -Al<sub>2</sub>O<sub>3</sub> was prepared by drying  $\gamma$ -Al<sub>2</sub>O<sub>3</sub> (Alcoa) at 423 K, calcination at 1,173 K to get  $\delta$ -Al<sub>2</sub>O<sub>3</sub>, sequential incipient-to-wetness impregnation using aqueous Ni(NO<sub>3</sub>)<sub>2</sub>·6H<sub>2</sub>O (Merck) and Pt(NH<sub>3</sub>)<sub>4</sub>(NO<sub>3</sub>)<sub>2</sub> (Aldrich) solutions with an intermediate calcination at 873 K and a final calcination at 773 K. The BET surface area of 82 m<sup>2</sup> g<sup>-1</sup> was determined using a Micromeritics Flowsorb II-2300 apparatus. The details of the preparation procedure have been reported elsewhere [17].

### 2.2 Reaction Experiments

Reaction experiments were conducted using 4 mm-i.d. stainless steel tubular down-flow microreactors placed in the constant-temperature zone of a 2.4-cm i.d. tube furnace controlled to  $\pm 0.1$  K by a Shimaden FP-21 programmable controller. In all experiments, 25 mg of 250–422  $\mu$ m (40–60 mesh) fresh catalyst particles were diluted with inert  $\delta$ -Al<sub>2</sub>O<sub>3</sub> to a total bed weight of 250 mg. Silane-treated glass wool (Alltech) was used to hold the catalyst bed in a fixed position. Preliminary experiments showed that the stainless steel reactor, glass wool and  $\delta$ -Al<sub>2</sub>O<sub>3</sub> were inert under the conditions used. Catalyst particle size and gas space velocity are important factors affecting mass transport in a solid-catalyzed system. Particles of 250–422  $\mu$ m size were found to be sufficiently small for avoiding internal diffusion effects under the present reaction conditions [18]. Experiments at constant contact time but varying gas flows with the same composition showed that external mass transfer effects were insignificant. In order to eliminate axial dispersion, the  $D_{\text{tube}}/D_{\text{particle}} > 10$  and  $L_{\text{bed}}/D_{\text{particle}} > 50$  criteria were also satisfied [19].

Nitrogen and hydrogen flows were regulated by Omega Model 5878 and Aalborg GFC171S series mass flow controllers, respectively. Liquid reactants were premixed according to the water/ethanol ratio specified, and the liquid mixture was introduced at constant flow rate using a Jasco PU-1580 intelligent HPLC pump into a stream of diluent nitrogen flow. The mixing section and the

connecting lines to the reactor were kept at 423 K by a heating tape plus temperature controller system for achieving evaporation and avoiding condensation. The liquid flow rate metered on the HPLC pump was converted into total and individual gas flow rates by assuming ideal gas behavior and utilizing water/ethanol ratios, molecular weights and liquid densities [17].

The catalyst was reduced under  $20 \text{ cm}^3 \text{ min}^{-1}$  pure hydrogen flow at 773 K for 4 h prior to each reaction experiment. After reduction, the reactor temperature was raised to the reaction temperature (623, 673, 723, 773 or 823 K) under inert nitrogen flow, and nitrogen was trapped within the reactor for 2 h while the reactant flow rates that were diverted to the bypass line reached steady-state. The feed composition and residence time were adjusted to give water/ethanol molar ratios of 3.0–6.0 (corresponding to steam-to-carbon ratios of 1.5–3.0) and  $W/F_{\text{Eo}}$  values of 2.8–5.2 ( $\text{mg s } \mu\text{mol}^{-1}$ ), respectively.

Product samples were collected and analyzed 1.5, 3, 4 and 5.5 h after the reaction mixture was introduced into the microreactor. Ethanol and other hydrocarbons were analyzed using a Shimadzu GC-14A gas chromatograph with a TCD, a Porapak Q column and He as carrier gas. A Shimadzu-8A gas chromatograph with a TCD, a Molecular Sieve 5A column and Ar as the carrier gas was used for analyzing  $\text{H}_2$  and CO.

In kinetic experiments, 20–25 mg fresh 0.2 wt%Pt–15 wt%Ni/ $\delta\text{-Al}_2\text{O}_3$  samples were diluted with  $\delta\text{-Al}_2\text{O}_3$  to a total bed weight of 250 mg. A temperature of 673 K was selected for kinetic analysis in the initial rates range using different feed concentrations. Various water/ethanol molar ratios in the range of 3.0–6.0 and  $W/F_{\text{Eo}}$  values of 0.90–3.70 ( $\text{mg s } \mu\text{mol}^{-1}$ ) were used in duplicate experiments with feed having ethanol mole fractions between 0.05 and 0.15. The temperature dependence of the rate constant and the activation energy were calculated by repeating these experiment sets at 698 and 723 K.

### 3 Results and Discussion

#### 3.1 Effect of Temperature

Considering the stoichiometry of Reaction 1, and in order to eliminate coke deposition on the Pt–Ni catalyst, the water/ethanol molar ratio was fixed at 5.0 for investigating the effect of temperature on ethanol conversion and product distribution. Figure 1 shows the notable effect of reaction temperature on ethanol conversion. The lowest conversion (ca. 12%) was obtained at 623 K whereas the highest one (ca. 100%) was achieved at 823 K. The most significant difference among the conversion levels in the same reaction time zone was observed in going from 723 to

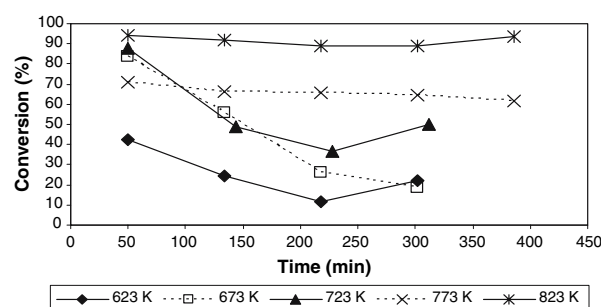


Fig. 1 Effect of temperature on ethanol conversion

773 K at around 230 min, which may be explained by considering possible side reactions, i.e. Reactions 2, 3 or 4. The production rates of two competing products, hydrogen and methane, are plotted in Fig. 2. Hydrogen production increases remarkably with increasing temperature from about  $40 \mu\text{mol/g cat-s}$  at 623 K to about  $185 \mu\text{mol/g cat-s}$  at 823 K while the highest methane production of ca.  $8 \mu\text{mol/g cat-s}$  is observed at 723 K as compared to ca.  $4 \mu\text{mol/g cat-s}$  at 623 K. These results, when combined with the data on  $\text{CO}_2$  and CO production rates (Fig. 3), suggest that ethanol SR with methane formation becomes

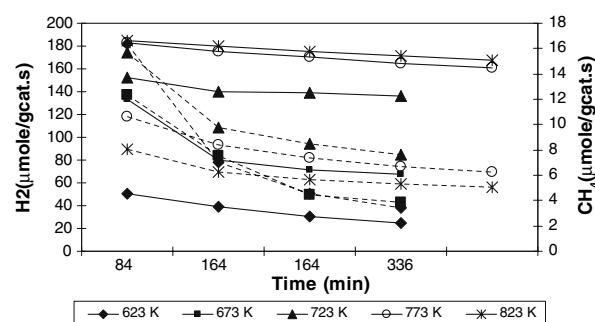


Fig. 2 The variation of hydrogen and methane production rates with temperature (solid lines and left y-axis represent  $\text{H}_2$  production, dotted lines and right y-axis represent  $\text{CH}_4$  production)

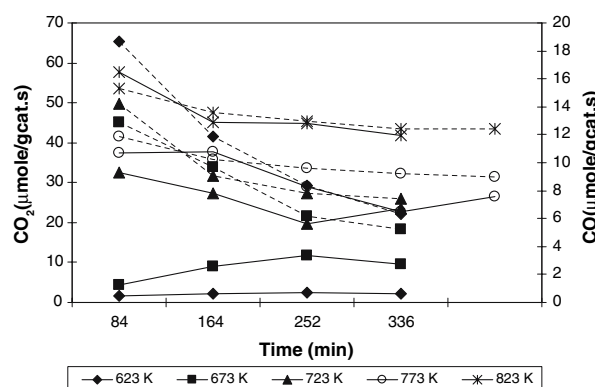
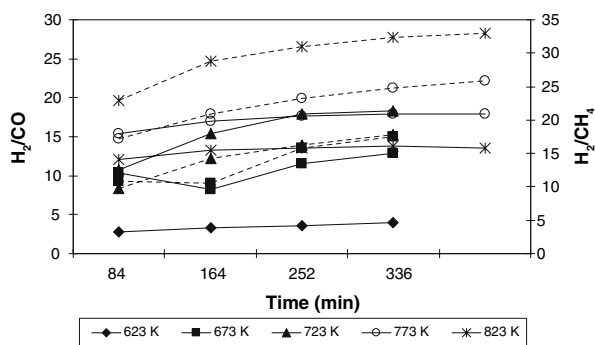


Fig. 3 The variation of carbon dioxide and carbon monoxide production rates with temperature (solid lines and left y-axis represent  $\text{H}_2$  production, dotted lines and right y-axis represent  $\text{CH}_4$  production)

significant at 723 K, since  $\text{CH}_4$ ,  $\text{H}_2$  and  $\text{CO}_2$  productions are all favored (Reaction 2).  $\text{CO}$ ,  $\text{CO}_2$  and  $\text{CH}_4$  production trends as well as the  $\text{H}_2/\text{CH}_4$  ratios (Figs. 2–4) at this temperature do not suggest significant methanation. At 823 K,  $\text{CH}_4$  production decreases while  $\text{CO}$  and  $\text{H}_2$  productions increase, indicating that the effluent composition may be affected by the thermodynamic equilibrium of methane steam reforming (Reaction 4). Furthermore, considering that mainly  $\text{CO}$  rather than  $\text{CO}_2$  is produced at 623 K (Fig. 3), together with  $\text{H}_2$  and some  $\text{CH}_4$ , it may be said that ethanol decomposition is significant at this temperature. The reaction mechanisms suggested at these temperatures coincide well with the overall reaction scheme proposed by Comas et al. [7] for bio-ethanol SR over monometallic  $\text{Ni}/\text{Al}_2\text{O}_3$ .

It is evident that hydrogen production should be as high as possible at the optimum reaction temperature. Figure 2 indicates maximum  $\text{H}_2$  production at 823 K; however, this is also the temperature at which maximum  $\text{CO}$  production occurs. Since  $\text{CO}$  acts as a poison for fuel cell electrodes, the level of  $\text{CO}$  in the reformer effluent has to be minimized. Therefore, optimum reaction temperature must be selected on the basis of the  $\text{H}_2/\text{CO}$  production ratio, i.e. the point selectivity for  $\text{H}_2$  (Fig. 4), rather than the hydrogen production rate. In this respect, 723 and 773 K stand out as better reaction temperatures than 823 K. The  $\text{H}_2/\text{CH}_4$  point selectivity is also important, since  $\text{CH}_4$  is an undesired byproduct that uses up hydrogen.  $\text{CH}_4$  production rate is highest at 723 K and decreases as the temperature is raised to 823 K (Fig. 2) with the highest  $\text{H}_2/\text{CH}_4$  point selectivity occurring at 823 K.

The selectivity data are also in good agreement with the reaction scheme outlined above. For instance, at 723 K, the high  $\text{H}_2$  and the low  $\text{CO}$  levels resulting from Reaction 2 lead to a high  $\text{H}_2/\text{CO}$  production ratio whereas at 823 K, since both  $\text{CO}$  and  $\text{H}_2$  are produced by Reaction 4, the selectivity stays at a relatively lower value.  $\text{CH}_4$  steam



**Fig. 4** Effect of temperature on hydrogen to carbon monoxide and hydrogen to methane selectivity's (solid lines and left y-axis represent  $\text{H}_2/\text{CO}$  selectivity, dotted lines and right y-axis represent  $\text{H}_2/\text{CH}_4$  selectivity)

reforming, which was suggested to be dominant at 823 K, causes the  $\text{H}_2/\text{CH}_4$  point selectivity to be the highest at this temperature; on the contrary,  $\text{CH}_4$  production from ethanol steam reforming at 723 K gives a much lower selectivity. As a result, the optimum reaction temperature may be proposed as 773 K, since both  $\text{CO}$  and  $\text{CH}_4$  production rates are relatively low while that of  $\text{H}_2$  is remarkably high ( $185 \mu\text{mol/g cat}\cdot\text{s}$ ).

### 3.2 Effect of Water/Ethanol Ratio

The effect of the water/ethanol molar ratio (W/E) on the steam reforming performance of  $\text{Pt-Ni}/\delta\text{-Al}_2\text{O}_3$  was studied at two temperatures, 673 and 773 K. No coke formation was observed at either temperature and even at the lowest water/ethanol ratio of 3.0 corresponding to a steam/carbon ratio of 1.5, which is well below the limit claimed to eliminate coke deposition over monometallic Ni catalysts. The resistance of bimetallic Pt-Ni to coke formation under these conditions may be explained by the presence of Pt despite its low weight percentage. The variation in total ethanol conversion with the water/ethanol ratio at 773 K is presented in Fig. 5, while the corresponding hydrogen and methane production trends are shown in Fig. 6. Ethanol conversion and hydrogen production are both improved by increasing the water/ethanol ratio from 5.0 to 6.0. On the contrary,  $\text{CH}_4$  production is suppressed with increasing W/E ratios, suggesting that methane reforming may be promoted at water/ethanol ratios greater than 4.0.

### 3.3 Kinetics of Ethanol Steam Reforming over $\text{Pt-Ni}/\delta\text{-Al}_2\text{O}_3$

The general form of the empirical power-function rate expression for ethanol conversion by steam reforming is postulated as follows:

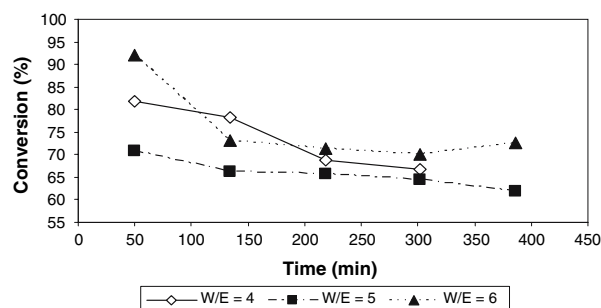


**Fig. 5** Effect of water to ethanol ratio on ethanol conversion

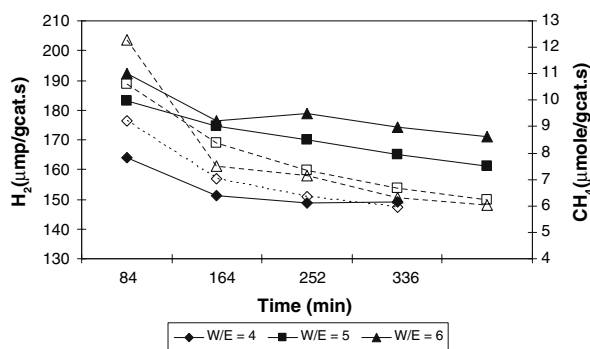


**Fig. 6** The variation of hydrogen and methane production rates with water to ethanol ratio (solid lines and left y-axis represent  $H_2$  production, dotted lines and right y-axis represent  $CH_4$  production)

$$-r_{C_2H_5OH} = \left[ k_0 \exp\left(-\frac{E_A}{RT}\right) \right] (P_{C_2H_5OH})^\alpha (P_{H_2O})^\beta \quad (5)$$

Evaluation of the rate parameters, i.e.  $\alpha$ ,  $\beta$ ,  $k_0$  and  $E_A$ , involves the calculation of reaction rates from ethanol conversion versus residence time data. Representative initial rate data obtained from duplicated experiments conducted at 673 K are presented in Table 1 along with the corresponding reactant partial pressures in the feed. Reaction orders were estimated using Eq. 5 and non-linear regression analysis in the MATLAB<sup>TM</sup> environment (Table 2). The effect of products was neglected since data were collected in the initial rates region. Reaction orders show that the rate of ethanol steam reforming is directly proportional to the partial pressure of ethanol and is mildly inhibited by steam partial pressure. These results are in agreement with previous research on steam reforming of ethanol over Ni-based catalysts in so far as a positive

**Table 1** Representative initial rate data over Pt–Ni/ $\delta$ - $Al_2O_3$  (673 K and 1 atm)

Experiment No.	W/F <sub>E0</sub> (mg s $\mu$ mol <sup>-1</sup> )	C <sub>2</sub> H <sub>5</sub> OH (kPa)	H <sub>2</sub> O (kPa)	N <sub>2</sub> (kPa)	Rate ( $\times 10^3$ mol gcat <sup>-1</sup> s <sup>-1</sup> )
1	2.932	5.05	25.25	70.70	0.0348
2	3.665	5.05	25.25	70.70	0.0518
3	1.466	8.42	33.67	58.92	0.0428
4	1.833	8.42	33.67	58.92	0.0479
5	1.955	6.31	37.88	56.81	0.0354
6	2.443	6.31	37.88	56.81	0.0479
7	0.978	11.22	37.41	52.37	0.0569
8	1.222	11.22	37.41	52.37	0.0582
9	1.173	9.35	41.15	50.50	0.1415
10	1.466	9.35	41.15	50.50	0.1535
11	1.173	10.52	31.56	58.92	0.1662
12	1.466	10.52	31.56	58.92	0.1317

**Table 2** Kinetic parameters of ethanol steam reforming (673–723 K)

Parameter	Units	Estimates
$k_0$	mol gcat <sup>-1</sup> s <sup>-1</sup> kPa <sup>-1.07</sup>	0.013
$E_A$	kJ mol <sup>-1</sup>	39.3 ( $\pm 2.1$ )
$\alpha$		1.25 ( $\pm 0.05$ )
$\beta$		-0.215 ( $\pm 0.015$ )

reaction order close to unity is observed for ethanol [9, 11]. The mechanism proposed for ethanol SR over Ru/ $Al_2O_3$  with excess water [12] implicates a surface complex between adsorbed ethanol and water from the gas phase, and the decomposition of this complex is taken as rate limiting to explain the first order dependence on ethanol. The reaction orders obtained in the present study would indicate a reaction occurring on a surface that is mostly covered by adsorbed water with relatively weak ethanol adsorption. The dependence of ethanol steam reforming rates on steam partial pressure has not been sufficiently addressed in the literature; however, the negative dependence observed in this study is in line with general trends observed in steam reforming of alkanes [17].

The last four data sets reported in Table 1 for ethanol SR at 673 K were repeated in duplicate at 698 and 723 K, in order to estimate the apparent activation energy ( $E_A$ ) and the pre-exponential factor ( $k_0$ ). These data are plotted in Fig. 7 and the parameter estimates are given in Table 2. The  $E_A$  value of  $39.3 \pm 2.1$  kJ mol<sup>-1</sup> is not in agreement with those reported in the literature for ethanol steam reforming on Ni-based catalysts but is comparable with  $E_A$  values for steam reforming of alkanes [17, 19]; furthermore, its magnitude confirms that kinetic experiments were conducted under reaction-controlling conditions. The low  $E_A$  values reported in the literature for ethanol SR and their irregularity [9–11] indicate that external and/or internal diffusion effects may be significant under the experimental conditions used in those studies.

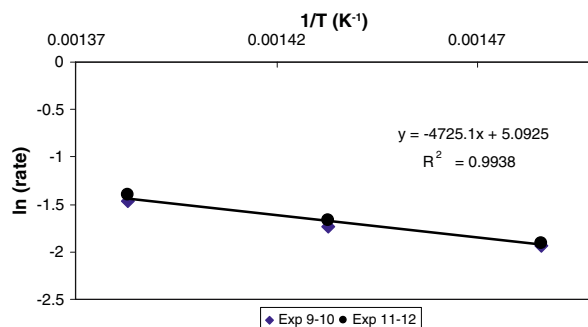


**Fig. 7** Arrhenius plot of ethanol steam reforming over Pt–Ni/ $\delta$ - $Al_2O_3$  (1 atm)



## 4 Conclusions

Ethanol steam reforming was studied at 673–723 K over bimetallic Pt–Ni/ $\delta$ -Al<sub>2</sub>O<sub>3</sub>, which is a successful IPOX catalyst with potential for use in fuel processors. The parametric study conducted indicates that the Ni-based bimetallic catalyst is resistant to coke deposition even at a steam-to-carbon ratio as low as 1.5 (W/E = 3.0); higher water-to-ethanol ratios have a positive effect on both ethanol conversion and H<sub>2</sub> formation. About 773 K is selected as the optimum reaction temperature, since high H<sub>2</sub> production rates are accompanied by low CO and CH<sub>4</sub> production rates, thus yielding favorable H<sub>2</sub>/CO and H<sub>2</sub>/CH<sub>4</sub> production ratios at this temperature. An empirical power function rate equation is proposed on the basis of intrinsic rates evaluated at 673 K over Pt–Ni/ $\delta$ -Al<sub>2</sub>O<sub>3</sub>. Reaction orders are calculated as 1.25 ( $\pm 0.05$ ) and  $-0.215$  ( $\pm 0.015$ ) with respect to ethanol and steam, respectively. The apparent activation energy and the pre-exponential factor between 673 and 723 K are found to be 39.3 ( $\pm 2.1$ ) kJ mol<sup>-1</sup> and 0.013 mol g cat<sup>-1</sup> s<sup>-1</sup> kPa<sup>-1.07</sup>, respectively.

**Acknowledgments** The financial support for this research was provided by TUBITAK-MAG through project 104M163 and by Boğaziçi University Research Fund through projects BAP-06HA501 and DPT-03K120250. TUBA-GEBIP grant to A.E. Aksoylu is gratefully acknowledged.

## References

1. Ralph TR, Hards GA (1998) Chem Ind 9:337
2. Ralph TR (1999) Plat Met Rev 43:14
3. Cheekatamarla PK, Finnerty CM (2006) J Power Sources 160:490
4. Trimm DL, Önsan ZI (2001) Catal Rev Sci Eng 43:31
5. Liguras DK, Goundani K, Verykios XE (2004) J Power Sources 130:30
6. Marino F, Boveri M, Baronetti G, Laborde M (2001) Int J Hydrogen Energy 26:665
7. Comas J, Marino F, Laborde M, Amadeo N (2004) Chem Eng J 98:61
8. Fatsikostas AN, Verykios XE (2004) J Catal 225:439
9. Sun J, Wu F, Qiu X-P, Zhu W-T (2005) Int J Hydrogen Energy 30:437
10. Akande A, Aboudheir A, Idem R, Dalai A (2006) Int J Hydrogen Energy 31:1707
11. Vaidya PD, Rodrigues AE (2006) Chem Eng J 117:39
12. Vaidya PD, Rodrigues AE (2006) Ind Eng Chem Res 45:6618
13. Avci AK, Önsan ZI, Trimm DL (2001) Appl Catal A Gen 216:243
14. Örücü E, Karakaya M, Avci AK, Önsan ZI (2005) J Chem Technol Biotechnol 80:1103
15. Ma L, Trimm DL (1996) Appl Catal A Gen 138:265
16. Caglayan BS, Avci AK, Önsan ZI, Aksoylu AE (2005) Appl Catal A Gen 280:181
17. Avci AK, Trimm DL, Aksoylu AE, Önsan ZI (2004) Appl Catal A Gen 258:235
18. Akin AN, Önsan ZI (1997) J Chem Technol Biotechnol 70:304
19. Kapteijn FGB, Marin JA, Moulijn JA (1999) Catalytic reaction engineering. In: van Santen RA, van Leeuwen PWNM, Moulijn JA, Averill BA (eds) Catalysis: an integrated approach, Elsevier, Amsterdam, pp 375–430